Supporting Information

Pandit et al. 10.1073/pnas.0907635106

SI Experimental Procedures

Expression, Purification, and Crystallization. The coding region for amino acids 215–900 of human PDE2A1 (GenBank NM_002599.3) was expressed in Sf21 insect cells with an in-frame C-terminal thrombin protease site, a biotin acceptor peptide tag, and 6×His tag. Cell lysate (in 50 mM Tris pH8.0, 50 mM NaCl, 2 mM TCEP, 10 μg/mL E-64, 1 μg/mL pepstatin, and 1 mM PMSF) was subjected to Ni^{2+} affinity chromatography, followed by thrombin cleavage to remove the tags, followed by a second Ni^{2+} affinity step. The flow-through from the last step was loaded onto a Mono-Q column in 50 mM Tris pH8.0, 20 mM NaCl and 2 mM TCEP, and PDE2A1 was eluted with a gradient to 50 mM Tris pH 8.0, 500 mM NaCl, and 2 mM TCEP.

Purified protein was exchanged into crystallization buffer (50 mM HEPES, pH 7.5, 50 mM NaCl, and 2 mM TCEP) to a final concentration of 10 mg/mL, mixed 1:1 with precipitant solution composed of 5–10% isopropanol, 0.1 M Mes, pH 5.4–6.0, 0.2 M $Ca(OAc)_2$, and set up in hanging drops. All purification and crystallization was carried out at 4 °C. Clusters of thin plate-like crystals appeared in 3–4 days, which were transferred to a cryoprotectant solution made up of the reservoir solution with 30% ethylene glycol, and flash-frozen by dipping into liquid nitrogen.

The catalytic domain, amino acids 579–919, of human PDE2A1 was expressed in Sf21 insect cells with an N-terminal 6×His tag and thrombin protease site. Purification followed the same protocol as described above for PDE2A (215–900), except that all buffers had 10% glycerol added.

Catalytic domain (579–919) purified protein was concentrated to 10 mg/mL and exchanged into crystallization buffer (25 mM HEPES pH 7.5, 25 mM NaCl, 2 mM TCEP, 10 μg/mL E-64, and 1 μg/mL pepstatin). Apo crystals were grown by hanging drop vapor diffusion at both room temperature and 4 °C over a precipitant solution comprised of 20% PEG 3350 and 0.2 M tri-sodium citrate.

For co-crystals with IBMX, the protein was concentrated with 1 mM IBMX in the crystallization buffer. The precipitant solution was 25% PEG 3350, 0.1 M Tris, pH 8.5, and 0.2 M $MgCl_2$. Clusters of needle-like crystals appeared, which were crushed and used as seeds to get diffraction quality crystals.

X-Ray Structure Determination and Refinement. X-ray diffraction data for PDE2A (215–900) crystals were collected at the microfocus beamline ID14 at ESRF Grenoble, with the wavelength tuned to the Zn absorption edge (1.28 Å). The structure was solved by molecular replacement, using structures of the individual subdomains as search models in the program PHASER (1). Weak rotation and translation solutions for the catalytic domains were found initially. The two highest peaks (>10 sigma) in anomalous difference Fourier maps calculated using phases from just the two catalytic domains were at the known Zn^{2+}-binding sites in the catalytic domains, which gave us additional confidence as to the correctness of the molecular replacement solution. This solution also allowed us to define the noncrystallographic symmetry axis. Additional searches in PHASER, keeping the two catalytic domains fixed and using the GAF-A domain from mouse PDE2A structure (PDB ID: 1mc0) as a search model led to solutions for the GAF-A domains. Electron density maps calculated by combining Zn-SAD phases to 6.5 Å resolution with phases calculated from a partial model comprised of the two GAF-A domains and two catalytic domains clearly defined the envelop of the missing GAF-B domains. After solvent flattening and averaging using "dm" and SOLOMON (2, 3), the maps were sufficiently improved to allow the GAF-B domains to be fit manually. This model was iteratively refined and rebuilt using BUSTER (4) and O (5), keeping tight noncrystallographic symmetry restraints throughout.

X-ray diffraction data for the catalytic domain crystals was collected at beamline ID17 at the Advanced Photon Source (APS), Argonne. Data collection and refinement statistics for all three structures are presented in Table S1. Both catalytic domain structures were solved by molecular replacement using the previously reported structure of hPDE2A catalytic domain (PDB ID: 1Z1L), and refined using refmac5 (6) in the CCP4 suite of programs (7).

1. McCoy AJ, et al. (2007) Phaser crystallographic software. *J Appl Crystallogr* 40:658–674.
2. Abrahams JP, Leslie AGW (1996) Methods used in the structure determination of bovine mitochondrial F1 ATPase. *Acta Crystallogr D Biol Crystallogr* 52:30–42.
3. Cowtan KD (1994) 'dm': An automated procedure for phase improvement by density modification. *Joint CCP4 and ESRF-EACBM Newsletter on Protein Crystallography* 31:34–38.
4. Blanc E, et al. (2004) Refinement of severely incomplete structures with maximum likelihood in BUSTER-TNT. *Acta Crystallogr D* 60:2210–2221.
5. Jones TA, Zou JY, Cowan SW, Kjeldgaard M (1991) Improved methods for building protein models in electron density maps and the location of errors in these models. *Acta Crystallogr A* 47:110–119.
6. Murshudov GN, Vagin AA, Dodson EJ (1997) Refinement of macromolecular structures by the maximum-likelihood method. *Acta Crystallogr D Biol Crystallogr* 53:240–255.
7. Bailey S (1994) The CCP4 suite: Programs for protein crystallography. *Acta Crystallogr D Biol Crystallogr* 50:760–763.
8. Kabsch W, Sander C (1983) Dictionary of protein secondary structure: Pattern recognition of hydrogen-bonded and geometrical features. *Biopolymers* 22:2577–2637.
9. Huai Q, Liu Y, Francis SH, Corbin JD, Ke H (2004) Crystal structures of phosphodiesterases 4 and 5 in complex with inhibitor 3-isobutyl-1-methylxanthine suggest a conformation determinant of inhibitor selectivity. *J Biol Chem* 279:13095–13101.
10. Huai Q, et al. (2004) Crystal structure of phosphodiesterase 9 shows orientation variation of inhibitor 3-isobutyl-1-methylxanthine binding. *Proc Natl Acad Sci USA* 101:9624–9629.
11. Wang H, Liu Y, Chen Y, Robinson H, Ke H (2005) Multiple elements jointly determine inhibitor selectivity of cyclic nucleotide phosphodiesterases 4 and 7. *J Biol Chem* 280:30949–30955.

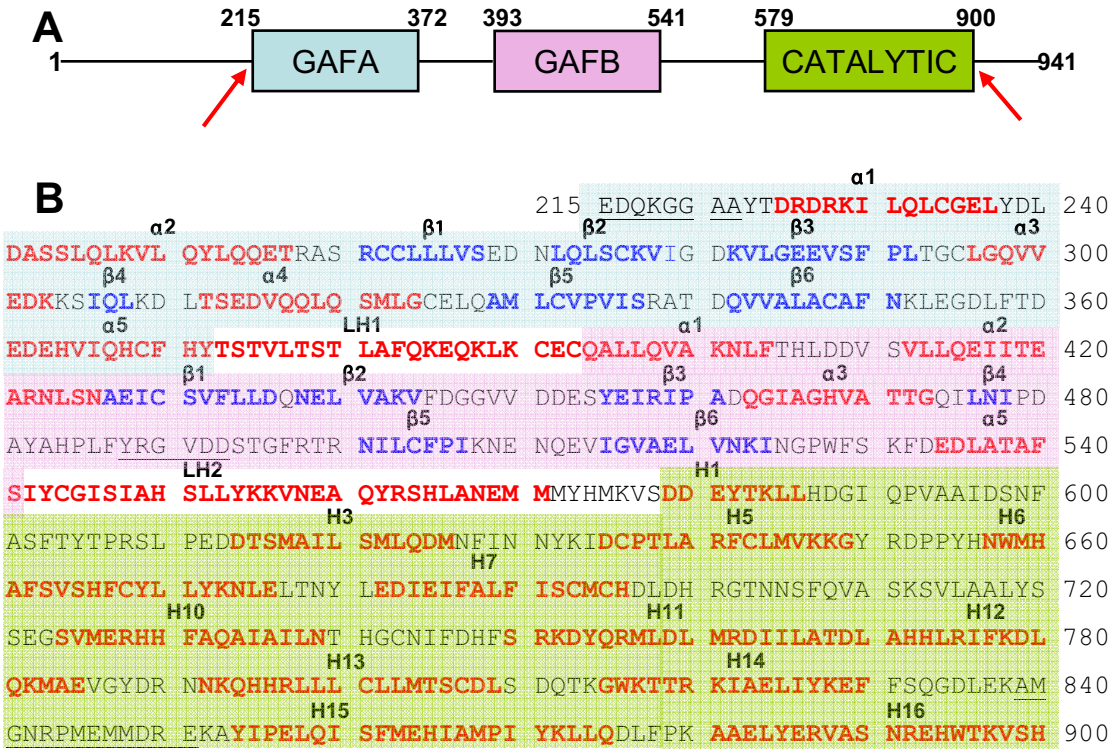

Fig. S1. Domain organization, sequence, and secondary structure of PDE2A. (*A*) PDE2 is a homodimer of 103 kDa subunits, each containing two GAF domains followed by a catalytic domain. By convention, the N-terminal GAF domain is called GAF-A, and the C-terminal domain is called GAF-B. The construct used for crystallization (residues 215–900, red arrows) encompasses both GAF domains and the catalytic domain. (*B*) The sequence of human PDE2A is shown, with the different domains colored as in panel *A*. Secondary structure assignments of molecule A following the convention of Kabsch and Sander (8) are indicated with red and blue bold-face letters for α-helices and β-sheets, respectively. Molecule B, which is related by a noncrystallographic 2-fold axis of symmetry, has the same secondary structure assignments. Residues that were not modeled into electron density because of disorder have been underlined.

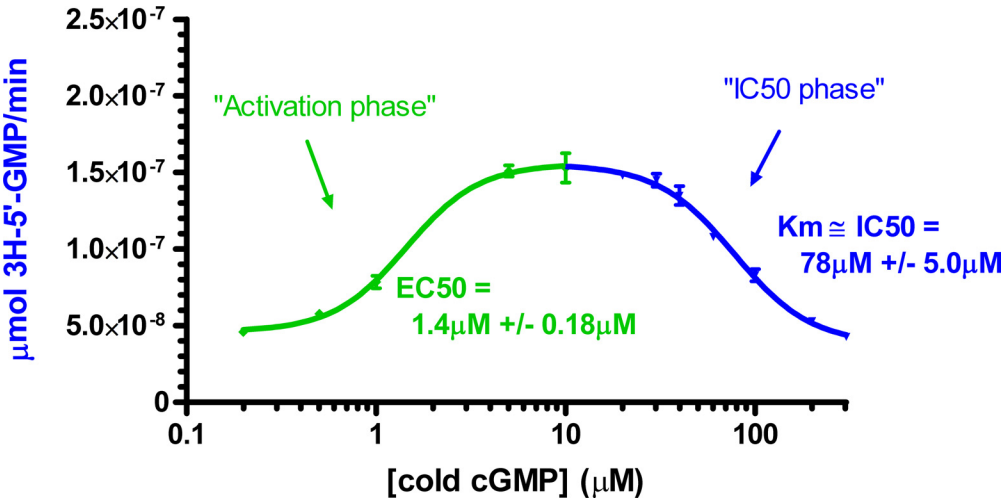

Fig. S2. Activation of PDE2 (215–900) by cGMP. PDE2A activity (cGMP hydrolysis) was measured at various concentrations (0–300 μM) of unlabeled (cold) cGMP, in the presence of 100 nM radiolabeled cGMP. The enzyme concentration was 1 nM. The data shown represent experiments performed three times. PDE2 enzyme assays were run in 50 mM Tris, 8.3 mM $MgCl_2$, and 0.05% BSA, in 384-well assay plates. Activity was measured by scintillation proximity assay, with the tritiated product 5′-GMP captured by yttrium silicate SPA beads and counted several hours later in a scintillation counter. For the activation experiment, a constant 100 nM ^{3}H-cGMP was paired with varying levels of cold cGMP (0–300 μM). Reactions were initiated by addition of enzyme and stopped by bead addition, at which point not more than 22% of substrate had been consumed. For purposes of determining background, every tested concentration of cold and hot cGMP was run with matching controls having the identical reagent concentrations, except for the addition of buffer in place of enzyme. Specific product cpm was then found by subtracting the background cpm at a given concentration of substrate from the corresponding raw number. No correction was made for isotope dilution.

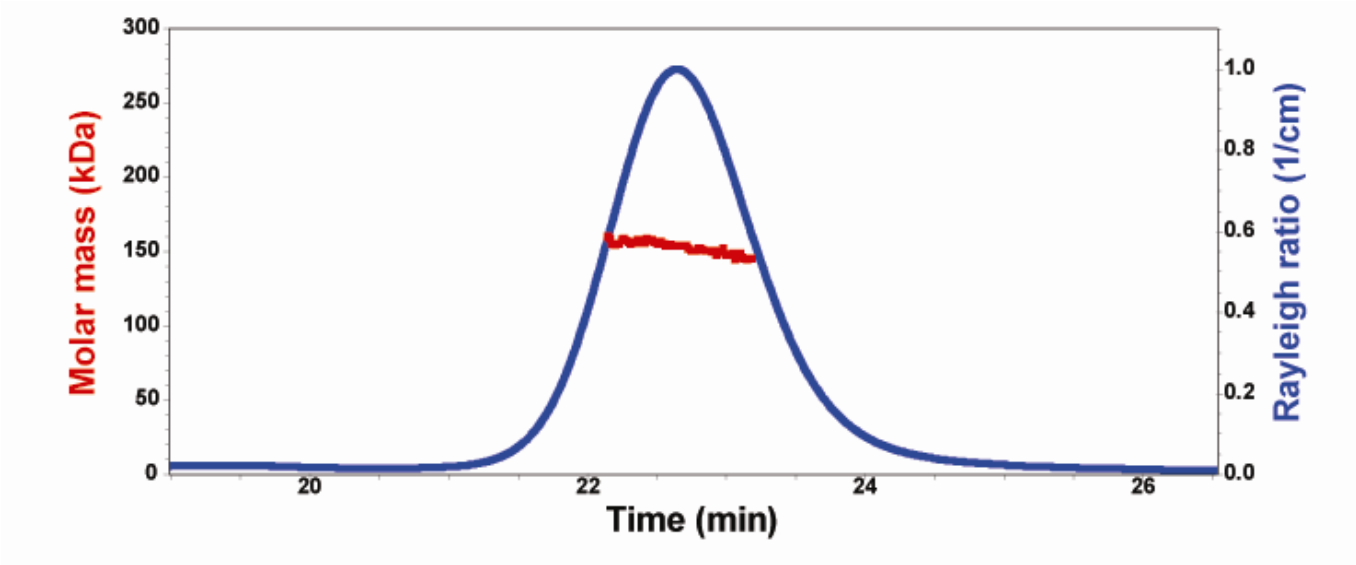

Fig. S3. PDE2A (215–900) is a dimer in solution. SEC-MALS data. The chromatogram is a Rayleigh Ratio trace (blue), and the linear trace within the chromatogram (red) represents mass distribution across the peak. The determined mass is 152 kDa (theoretical dimer is 163 kDa). Size exclusion chromatography with multiangle light scattering (SEC-MALS) was used to determine molecularity. Separation was performed using a model 1100 HPLC system (Agilent Technologies) with a 10/300 GL Superdex-200 SEC column (GE Healthcare). The HPLC was coupled to an Agilent 1100 diode array detector ($UV_{280\ nm}$), an Optilab rEX refractometer (Wyatt Technology), and a Wyatt Technology DAWN EOS 18-angle detector. The system was normalized with BSA (Thermo Scientific). Tris (50 mM), pH 8.0, 100 mM NaCl was the mobile phase, delivered at a flow rate of 0.5 mL/min. Four microliters 13 mg/mL protein was injected onto the column. Data analysis was performed using the Wyatt Technology Astra V software package.

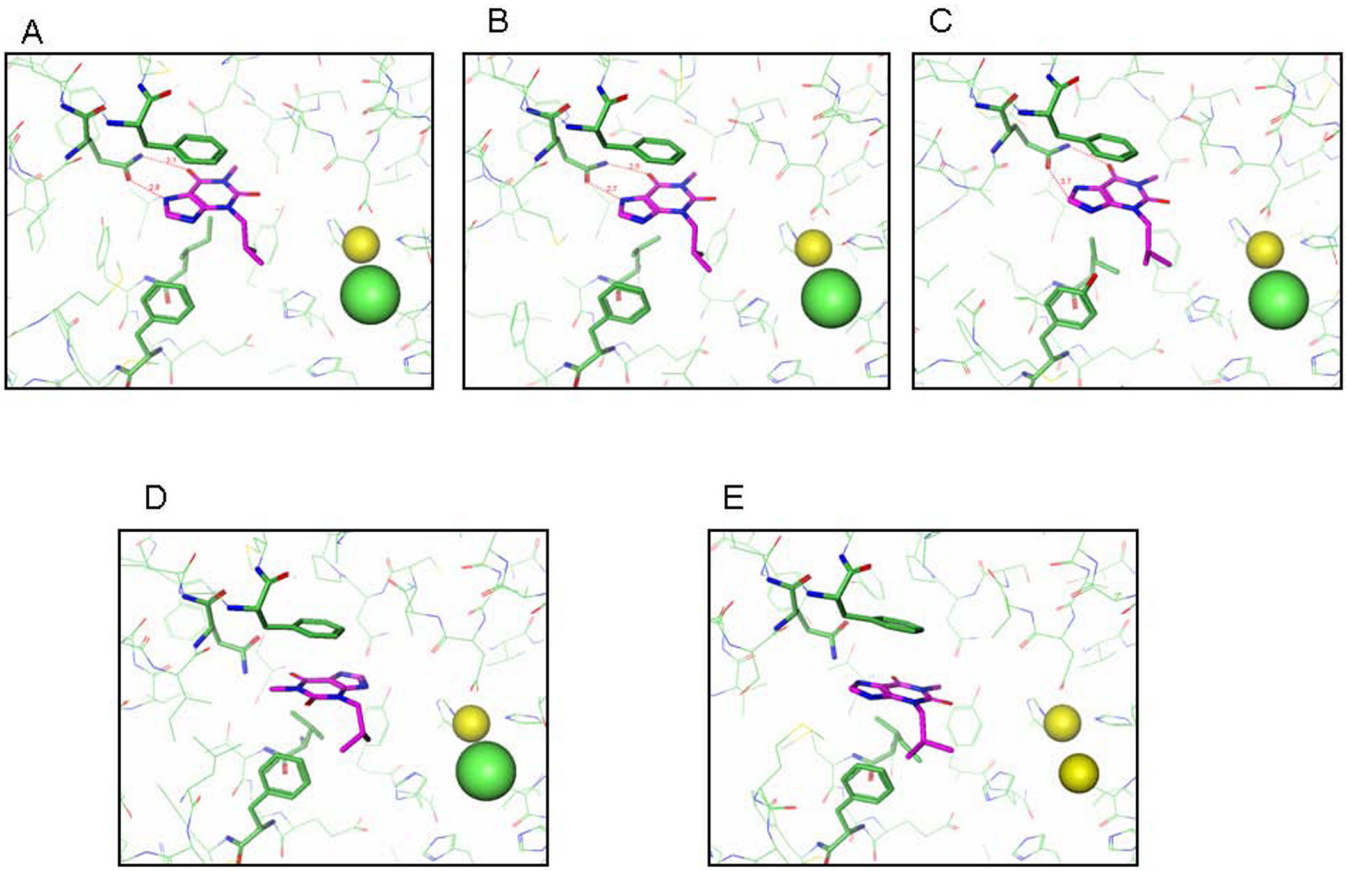

Fig. S4. Comparison of binding mode of IBMX in different PDE catalytic domains. (*A*) PDE2A (579–919, IBMX complex, this study); (*B*) PDE5A, (1RKP), (9); (*C*) PDE9A (2HD1), (10); (*D*) PDE7A (1ZKL), (11); (*E*) PDE4D (1RKO), (9). Catalytic domains are superimposed to minimize the r.m.s deviation between their Cα atoms, and all of the pictures have been made from exactly the same orientation. In each figure, metal ions are shown as spheres (Zn-yellow, Mg-green), key conserved residues, Q859, F862, I826, F830 (PDE2A numbering) are shown as green sticks, and IBMX is shown in purple sticks. Observed H-bonds are indicated with dashed lines. All water atoms have been hidden for clarity. IBMX binds to PDE2A in the same orientation as it does to the cGMP-specific PDEs 5 and 9, and in a completely different orientation compared with the cAMP specific PDEs 4 and 7. The conserved glutamine in the PDE2A (215–900) structure can thus be said to be in the ''cGMP-binding'' orientation.

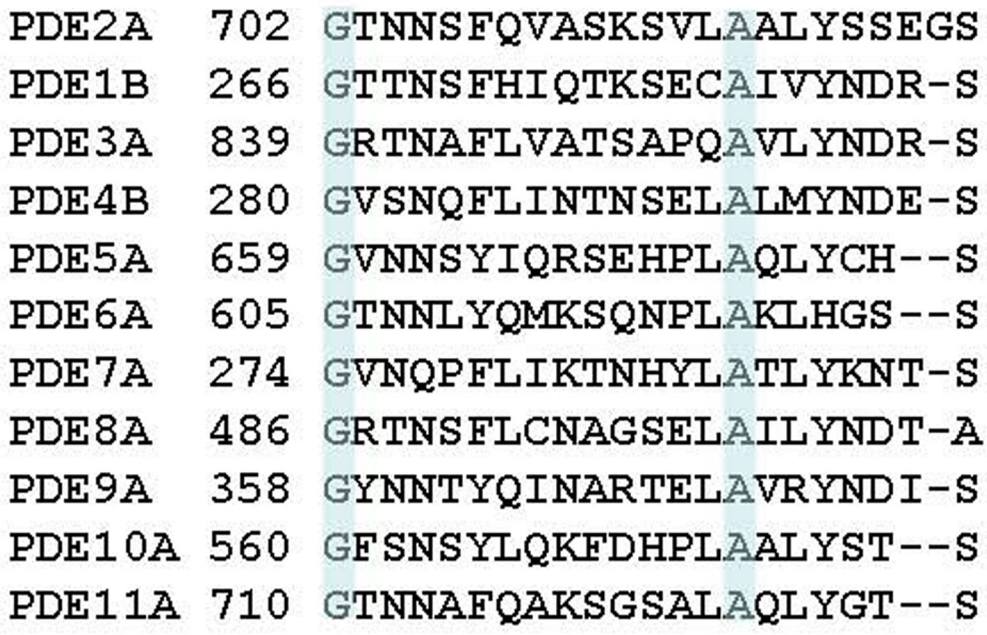

Fig. S5. Alignment of H-loop sequences from all phosphodiesterases, showing the conserved glycine and alanine residues at the two ends of the loop.

Table S1. X-ray data collection and refinement statistics

Data collection	PDE2 (215–900)	PDE2 (579–919) Apo	PDE2 (579–919) IBMX-complex
Space group	*P*212121	*P*6122	*P*1
Unit cell parameters			
a, Å	66.23	108.02	55.81
b, Å	89.70	108.02	73.29
c, Å	264.18	515.56	91.53
α, °	90.0	90.0	109.3
β, °	90.0	90.0	88.8
γ, °	90.0	120.0	89.0
Resolution, Å	3.0	2.5	1.6
Total measurements	453,133	352,113	426,212
Unique reflections	31,809	54,006	157,174
Completeness, %	99.8 (100)	84.3 (38.1)	83.9 (36.7)
Average I/σ	28.6 (2.4)	19.4 (2.2)	16.7 (1.6)
R_{merge}	0.14	0.09 (0.32)	0.11 (0.34)
Refinement			
Molecules in a.u.	2	4	4
R factor	0.21	0.23	0.17
R_{free}	0.31	0.29	0.23
rmsd			
Bond	0.011	0.033	0.029
Angle	1.38	2.0	2.25
Average B factor	77.6	43.3	22.7